

FAST COMPUTATION OF GEOMETRIC MOMENTS AND INVARIANTS USING SCHLICK'S APPROXIMATION

R. MUKUNDAN

*Department of Computer Science and Software Engineering
University of Canterbury, Christchurch, New Zealand
mukundan@canterbury.ac.nz*

Geometric moments have been used in several applications in the field of Computer Vision. Many techniques for fast computation of geometric moments have therefore been proposed in the recent past, but these algorithms mainly rely on properties of the moment integral such as piecewise differentiability and separability. This paper explores an alternative approach to approximating the moment kernel itself in order to get a notable improvement in computational speed. Using Schlick's approximation for the normalized kernel of geometric moments, the computational overhead could be significantly reduced and numerical stability increased. The paper also analyses the properties of the modified moment functions, and shows that the proposed method could be effectively used in all applications where normalized Cartesian moment kernels are used. Several experimental results showing the invariant characteristics of the modified moments are also presented.

Keywords: Geometric moments; moment invariants; fast computation of moments; Schlick's approximation.

1. Introduction

Moment functions computed from an image have been extensively used as invariant feature descriptors in applications involving pattern recognition, image classification and template matching.^{2,17} They have also been used to extract the primary geometrical attributes of an image shape for 2D pose estimation.¹¹ Among the class of moment functions, geometric moments have the simplest structure that has the form of a sum of intensities weighted by a monomial in image coordinates. They are therefore well suited for simple recognition tasks. Hu⁵ used theory of algebraic invariants to derive a set of geometric moment functions that are invariant with respect to translation, scaling as well as rotation. The capability of low-order geometric moments to represent both shape characteristics and invariant features of an image has led to the development of several new algorithms and applications.^{1,3,13} Research in the area of geometric moments have also spawned the study of similar moment functions with complex and orthogonal kernels for more accurate representation of image features.^{4,6,12,20,21}

An important aspect of the study of geometric moments is the analysis of their computational complexity and numerical stability. Even though geometric moments have a very simple kernel function when compared with complex moments and orthogonal moments, several methods have been proposed in the literature to speed up the computation of feature vectors containing several moment terms. Fast computation of moments is an important problem in real-time recognition, classification and retrieval systems. Certain applications may involve a large image data set,¹⁴ or a set of large images,¹⁰ or may require the computation of high-order moments.⁸ Algorithms for fast computation of geometric moments typically make use of properties of the moment integral such as separability. The two-dimensional moment integral can be reduced to a one-dimensional contour integral along a shape's boundary, using Green's theorem.^{7,19} The separability property has been effectively used in evaluating geometric moments using a quadtree decomposition,¹⁸ and a matrix based representation of the moment transform.⁹

Geometric moments evaluated at high orders tend to become numerically unstable due to the monomial structure of the kernel functions. Image coordinate values are usually normalized to a value less than 1 by dividing by the image size, in order to eliminate this problem. With coordinate normalization, moment values tend to zero instead of infinity as the moment order increases. Normalization also helps in reducing the sensitivity of moment functions to image noise. Computation of "normalized" moment kernels would not generally have any impact on the usability of such moments in a feature vector, since high order moments contain less important information about the shape they represent. However, moments using normalized coordinates will have to be computed using floating-point values, while the computation of regular geometric moments requires only integer additions and multiplications.

This paper presents a novel and highly efficient algorithm for fast computation of normalized geometric moments using Schlick's approximation for the kernel functions.¹⁵ The method presented here is distinctively different from previously researched methods in that it completely replaces the monomial kernel with another function which gives a result that closely matches that of geometric moments. With this approximation, repeated multiplication of coordinate values can be totally eliminated, leading to a significant reduction in the computational time required for the evaluation of each kernel function. The method presented in this paper does not affect the desirable properties (continuous differentiability, separability, symmetry, etc.) of the moment integral. Therefore, algorithms such as the application of Green's theorem that have been proposed for fast computation of geometric moments could still be used on the modified moments to further reduce the amount of computations. The paper presents the mathematical framework of the new class of geometric moments using Schlick's approximation. It also provides the derivation of translation and scale invariants of the modified moments. Experimental results are presented to show the advantages of the proposed method over conventional geometric moments.

The paper is organized as follows: the next section gives definition and basic properties of geometric moments with normalized coordinates. The Schlick's approximating function is introduced in Sec. 3. The modified moment definition based on Schlick's approximation is presented in Sec. 4. The computational advantages provided by the modified kernel functions are outlined in Sec. 5. Experimental results showing the desirable features of the proposed moment functions are given in Sec. 6. Section 7 summarises the ideas presented in this paper and discusses some possible extensions.

2. Geometric Moments

In this paper, we use the following definition of geometric moments of order $p + q$ of an image $I(x, y)$, $x, y = 0, 1, \dots, N - 1$:

$$m_{pq} = \sum_{x=0}^{N-1} \sum_{y=0}^{N-1} \hat{x}^p \hat{y}^q I(x, y), \quad p, q = 1, 2, 3, \dots \quad (1)$$

where \hat{x}, \hat{y} denote normalized image coordinates given by

$$\hat{x} = \frac{x}{N}; \quad \hat{y} = \frac{y}{N}, \quad \hat{x}, \hat{y} \in [0, 1). \quad (2)$$

Note that the above definition could be easily modified for nonsquare images of size $M \times N$ ($M \neq N$). We can extend the definition in (1) to include zero-order moments using the coordinate independent summation

$$m_{00} = \sum_{x=0}^{N-1} \sum_{y=0}^{N-1} I(x, y). \quad (3)$$

The image centroid (in normalized coordinates) is defined in terms of the first order moments as follows:

$$\hat{X} = \frac{m_{10}}{m_{00}}; \quad \hat{Y} = \frac{m_{01}}{m_{00}} \quad (4)$$

where according to (1),

$$m_{10} = \frac{1}{N} \sum_{x=0}^{N-1} \sum_{y=0}^{N-1} xI(x, y), \quad \text{and} \quad m_{01} = \frac{1}{N} \sum_{x=0}^{N-1} \sum_{y=0}^{N-1} yI(x, y).$$

The translation invariants for geometric moments are known as central moments, and they are computed by offsetting the image coordinates by the centroid values. With coordinate normalization, the central moments corresponding to Eq. (1) are given by

$$\mu_{pq} = \sum_{x=0}^{N-1} \sum_{y=0}^{N-1} (\hat{x} - \hat{X})^p (\hat{y} - \hat{Y})^q I(x, y). \quad (5)$$

The above definition leads to a very simple formula for translation+scale invariants:

$$\eta_{pq} = \frac{\mu_{pq}}{m_{00}}. \quad (6)$$

It may be noted here that the form of the invariant in (6) is different from Hu's scale invariants which require a division by $(m_{00})^{(p+q+2)/2}$. This is due to the normalization of image coordinates as in (2). Even though the fundamental geometric features such as area, centroid, and principal axes of an image shape can be extracted from moments of orders up to 3, higher order moment features are commonly used in recognition and classification systems. Algorithms for image reconstruction using geometric moments (or orthogonal moments expressed in terms of geometric moments) also require the evaluation of moments of a high order, depending on the image size. Computation of high-order geometric moments involves repeated multiplication of the coordinate values. Schlick's approximation of the term x^p with a simple function eliminates the need for this repeated operation, and significantly speeds up the computation of moment terms.

3. Schlick's Approximation

The Schlick's approximation of an exponential function x^p , $x \in [0, 1)$, is given by¹⁵

$$\begin{aligned} S_p(x) &= \frac{x}{x+p-xp}, & p \in [1, \infty), \\ &= 1, & \text{if } p = 0. \end{aligned} \quad (7)$$

The above formula is commonly used in Computer Graphics to approximate the term $(\cos \phi)^f$ that appears in the traditional Phong's illumination model for specular reflections,¹⁶ with a simple function that does not require exponentiation. Interestingly, $S_p(x)$ represents the ratio of a linear interpolation between 0 and 1 (given by x in the numerator) to a linear interpolation between p and 1 (given by $p(1-x) + x$ in the denominator), with x as the parameter for interpolation. Thus $S_p(x)$ has a value ranging from 0 to 1, for all p . Figure 1 shows that the function in (7) can be used as an approximation of the shape of x^p . It is also clear from the figure that Schlick's approximation provides a slower convergence to zero for $x < 1$, as the value of p is increased. This is particularly useful in moment based feature representation, as higher order moments can then contain some significant information.

Figure 2 shows the variation of the approximation error given by

$$E_p(x) = S_p(x) - x^p, \quad (8)$$

with respect to x for different values of p . In the following, we give a brief analysis of the maximum possible error value. The error function $E_p(x)$ is continuous and differentiable for $x \in [0, 1]$, $p > 0$. Equating the derivative of $E_p(x)$ to zero, we get the following condition for the error function to have an extremum value.

$$x^{p-1} = \frac{1}{(x+p-xp)^2}. \quad (9)$$

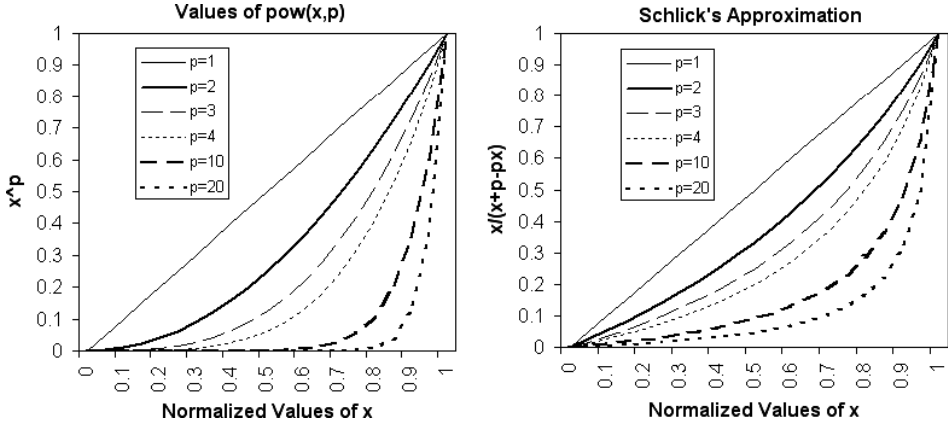


Fig. 1. Comparison of values of the function x^p and its Schlick's approximation for different values of p .

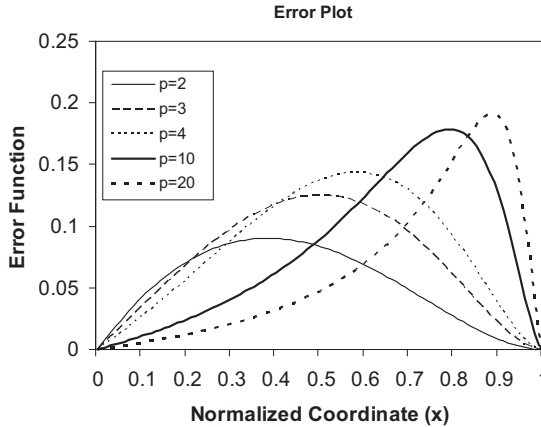


Fig. 2. Plots of the error function $E_p(x)$ for different values of p .

Clearly $x = 1$ is a common solution for the above equation, where the error function attains a minimum. As an example, if $p = 2$, the error function attains an extremum value when $x = (3 - \sqrt{5})/2$ and $x = 1$. Similarly, for $p = 3$, the maximum error occurs at $x = 0.5$. The point at which this maximum error occurs converges to the point $x = 1$ as p increases. It can be experimentally verified that the global maximum of the error function is 0.2.

4. Modified Moments: Definitions

We define a new set of modified geometric moments by approximating the kernel function in (1) by Schlick's formula:

$$\tilde{m}_{pq} = \sum_{x=0}^{N-1} \sum_{y=0}^{N-1} S_p(\hat{x}) S_q(\hat{y}) I(x, y), \quad p, q = 0, 1, 2, \dots \tag{10}$$

where \hat{x}, \hat{y} are given by (2). It is easy to see that the modified kernel $S_p(\hat{x})$ has the desirable properties of continuity and differentiability as the original kernel \hat{x}^p for $\hat{x} \in (0, 1)$ and $p \in [0, \infty)$. Further, we have the following uniqueness conditions:

$$\begin{aligned} S_p(x) = S_q(x) &\Rightarrow p = q \quad \text{for } x \in (0, 1), \quad \text{and } p, q > 0, \\ S_p(x) = S_p(y) &\Rightarrow x = y \quad \text{for } x, y \in (0, 1), \quad \text{and } p > 0. \end{aligned} \tag{11}$$

Assuming that the intensity function $I(x, y)$ is piecewise continuous and bounded with nonzero values only in a finite region of the xy -plane, moments \tilde{m}_{pq} of all orders exist and are finite.

We now consider the approximation of the exponential terms of the normalized central moments given in (5). We note here that the normalized central variables $(\hat{x} - \hat{X}, \hat{y} - \hat{Y})$ used in (5) have an extended range $[-1, 1]$. We correspondingly extend the Schlick's approximation function in Eq. (7), for $x \in (-1, 1)$ as follows:

$$\begin{aligned} S'_p(x) &= \frac{x}{x + p - xp}, \quad 0 \leq x < 1, \quad p \in [1, \infty), \\ S'_p(x) &= \frac{(-1)^p x}{x - p - xp}, \quad -1 < x < 0, \quad p \in [1, \infty), \\ S'_p(x) &= 1 = S_p(x), \quad \text{if } p = 0, \quad \text{for all } x. \end{aligned} \tag{12}$$

The above function satisfies the symmetry property given by

$$S'_p(-x) = (-1)^p S'_p(x). \tag{13}$$

Plots of the extended Schlick's function are given in Fig. 3.

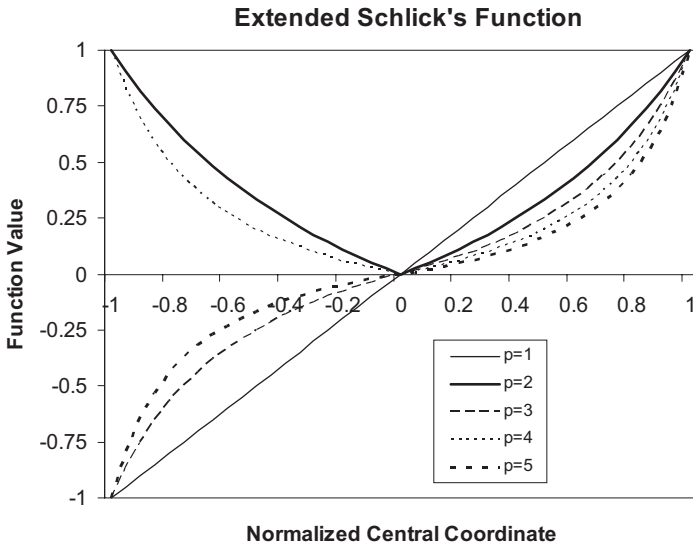


Fig. 3. Plots of the extended Schlick's function $S'_p(x)$ for different values of p .

The modified central moments invariant with respect to translation, are defined as follows:

$$\tilde{\mu}_{pq} = \sum_{x=0}^{N-1} \sum_{y=0}^{N-1} S'_p(\hat{x} - \hat{X}) S'_q(\hat{y} - \hat{Y}) I(x, y) \tag{14}$$

where \hat{x}, \hat{y} are given by (2), and \hat{X}, \hat{Y} by (4). The following properties are evident:

$$\begin{aligned} \tilde{m}_{00} = m_{00} = \mu_{00} = \tilde{\mu}_{00}; \quad \tilde{m}_{10} = m_{10}; \quad \tilde{m}_{01} = m_{01}; \quad \tilde{m}_{11} = m_{11} \\ \mu_{01} = \mu_{10} = \tilde{\mu}_{01} = \tilde{\mu}_{10} = 0. \end{aligned} \tag{15}$$

The translation + scale invariants of the modified moments can be obtained directly from (14) as

$$\tilde{\eta}_{pq} = \frac{\tilde{\mu}_{pq}}{m_{00}}. \tag{16}$$

As noted earlier, both Eqs. (6) and (16) differ from Hu’s scale invariants because of coordinate normalization.

5. Modified Moments: Computational Advantages

The primary advantage of Schlick’s approximation in the computation of moment terms (10), (14) is the elimination of the exponential term. This reduces the order of complexity in evaluating \hat{x}^p from $O(p)$ to $O(1)$. This also eliminates the need for precomputing the polynomial values and storing them in a two-dimensional array for evaluating moment functions. The moment kernel in both (10) and (11) is still separable, and any algorithm using this property could also be applied to the modified moments. For example, the evaluation of moments in (10) of orders up to $p = q = N$ for a $N \times N$ image could be carried out as follows, to reduce the order of complexity from $O(N^4)$ to $O(2N^3)$.

$$\begin{aligned} \varphi_p(x) &= \sum_{y=0}^{N-1} S_p(\hat{y}) I(x, y) \\ \tilde{m}_{pq} &= \sum_{x=0}^{N-1} S_p(\hat{x}) \varphi_p(x). \end{aligned} \tag{17}$$

Since the approximating function is both continuous and differentiable in the region $[0, 1)$, fast methods such as those based on Green’s theorem¹⁹ could be used to further reduce the amount of computation by converting two-dimensional moment integrals to one-dimensional contour integrals.¹³ Given a set of n edge points (\hat{x}_i, \hat{y}_i) , $i = 0, 1, \dots, n - 1$, forming a closed boundary of a binary image, its moments could be computed using Schlick’s approximation functions as

$$\tilde{m}_{pq} = \frac{1}{(p + 1)} \sum_{i=0}^{n-1} S_{p+1} \left(\frac{\hat{x}_{i+1} + \hat{x}_i}{2} \right) S_{q+1} \left(\frac{\hat{y}_{i+1} + \hat{y}_i}{2} \right) (\hat{y}_{i+1} - \hat{y}_i) \tag{18}$$

where $\hat{x}_n = \hat{x}_0$, and $\hat{y}_n = \hat{y}_0$.

The symmetry property (13) is useful in reducing the amount of computations by requiring the kernel to be evaluated only in one quadrant of the image space. Thus, we can rewrite (14) as follows:

$$\tilde{m}_{pq} = \sum_{x=0}^{(N/2)-1} \sum_{y=0}^{(N/2)-1} S'_p(\hat{x} - \hat{X})S'_q(\hat{y} - \hat{Y}) \times \left\{ I(x, y) + (-1)^p I(N - 1 - x, y) + (-1)^q I(x, N - 1 - y) + (-1)^{p+q} I(N - 1 - x, N - 1 - y) \right\}. \quad (19)$$

The completeness property of the moment kernel could be used to derive an inverse moment transform for image reconstruction. If $F(u, v)$ represents the Fourier transform of the image $I(x, y)$, then we can get a polynomial approximation of $F(u, v)$ in terms of moments up to order $N \max$ as³:

$$F(u, v) = \sum_{p=0}^{N \max} \frac{(-2i\pi)^p}{p!} \sum_{k=0}^p \binom{p}{k} u^{p-k} v^k m_{p-k,k}. \quad (20)$$

The amount of computation involved in the above process could be significantly reduced by using Schlick’s approximation functions:

$$F(u, v) = \sum_{p=0}^{N \max} \frac{(-2i\pi)^p}{p!} \sum_{k=0}^p \binom{p}{k} S_{p-k}(u)S_k(v)\tilde{m}_{p-k,k} \quad (21)$$

where \tilde{m}_{pq} is computed using (10), and $u, v \in [0, +1)$.

6. Experimental Results

The moment functions based on Schlick’s approximation proposed in the previous section were implemented and tested with a series of images to analyze their usefulness in moment based recognition tasks. The input set consisted of both binary and gray-level images (Fig. 4).

Figure 5 shows a comparison of moments m_{p2} , and \tilde{m}_{p2} ($q = 2$) computed for the “Aircraft” image, using Eqs. (1) and (10) respectively. This comparative analysis establishes the fact that the modified moments could be used in place of







					
“Ant” (200x200)	“Letter G” : (128x128)	“Aircraft” : (200x200)	“Tool” (120x120)	“Letter A” (100x100)	“Bird” (256x256)

Fig. 4. Test images used for comparative analysis.

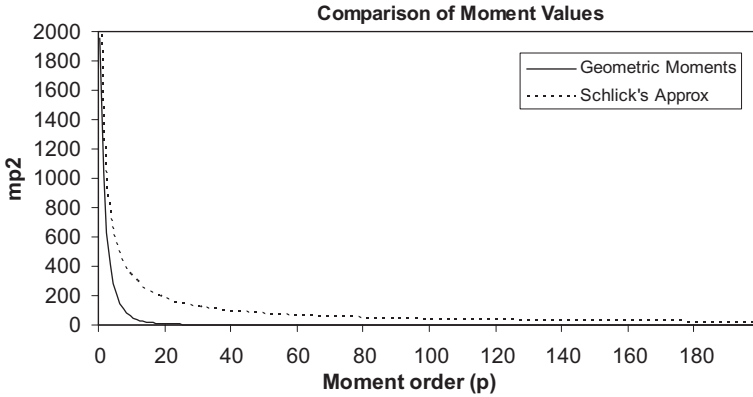


Fig. 5. Plots of geometric moments m_{p2} and the modified moments \tilde{m}_{p2} for various values of p , computed for the “Aircraft” image in Fig. 4.

geometric moments, without introducing noticeable errors. The slow convergence of moments \tilde{m}_{p2} to zero with increasing values of p , provides a better dynamic range of values of the modified moments compared to the original geometric moments. This property of the proposed moments may be useful in applications requiring higher order terms, particularly in pattern recognition using feature vectors consisting of high order moments.

The time required for evaluating moments of order p ($m_{p0}, m_{p-1,1}, m_{p-2,2}, \dots$) was analyzed with the value of p ranging from 0 to 100. The computations were performed on a 2.8 GHz Intel-Pentium-4 CPU with 1 GB of RAM. Figure 6 gives a comparison of CPU times with the values of x^p, y^q computed using (i) repeated

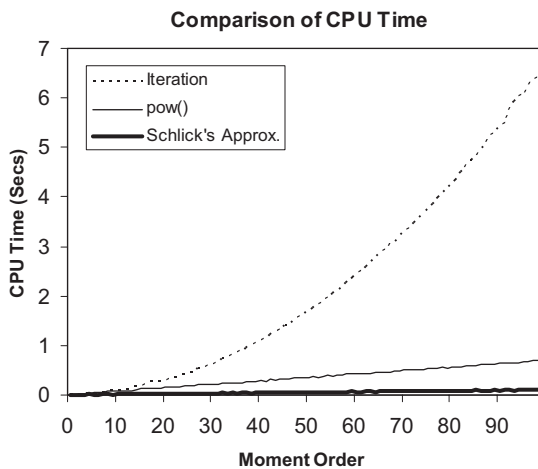


Fig. 6. Comparison of CPU times with the moment kernel computed using the exponential function and Schlick’s approximation.

multiplication, (ii) built-in “pow()” function and (iii) Schlick’s approximation. In all the three cases, the calculation of moment values was done using the straight forward direct-sum method. The computational time could be further reduced by using the separability property (17) and the symmetry property (19) of the kernel functions. Another way of reducing the time taken for moment calculations is by precomputing the values of the basis polynomials. Accessing one element from an array and computing a value of the Schlick’s approximation function both take $O(1)$ time. The results would be comparable with that obtained using Schlick’s approximation, but the proposed method eliminates the need for additional storage of polynomial values.

Coordinate normalization helps in reducing the sensitivity of the moments to input noise, and provides better invariants. Values of central moments computed using (5), (14) with the binary image “G” with the addition of 2% salt-and-pepper-noise, and translated to different positions, are given in Table 1.

A similar analysis was carried out with the gray-level image “Letter A”, with two different noise levels, and the results are tabulated in Tables 2 and 3. In all these experiments, moments computed using Schlick’s approximation have shown better invariance characteristics compared to normalized geometric moments.

Since each moment function has a different mean value, we used the coefficient of variation (ratio of the standard deviation to the mean expressed as a percentage)

Table 1. Translation invariants computed from the binary image “Letter G” with 2% noise.

Centroid		Geometric Moments			Schlick’s Approximation		
\hat{X}	\hat{Y}	μ_{12}	μ_{32}	μ_{40}	$\tilde{\mu}_{12}$	$\tilde{\mu}_{32}$	$\tilde{\mu}_{40}$
0.49	0.50	284.91	83.74	170.70	357.55	187.05	431.65
0.51	0.56	285.86	83.10	170.97	358.18	186.95	431.96
0.47	0.45	283.11	82.60	165.60	355.52	185.44	426.38
0.56	0.52	282.10	80.71	165.93	354.84	184.13	427.16
0.42	0.47	288.20	86.32	181.75	361.82	191.10	443.98
0.54	0.44	287.35	85.79	173.45	361.20	189.69	436.65
(SD/Mean)% >		0.83	2.49	3.46	0.80	1.39	1.51

Table 2. Translation invariants computed from the gray-level image “Letter A” with 5% noise.

Centroid		Geometric Moments			Schlick’s Approximation		
\hat{X}	\hat{Y}	μ_{20}	μ_{13}	μ_{42}	$\tilde{\mu}_{20}$	$\tilde{\mu}_{13}$	$\tilde{\mu}_{42}$
0.53	0.52	2140.75	567.23	254.32	2636.28	980.51	599.97
0.54	0.59	2132.29	564.52	250.10	2626.35	975.71	595.17
0.52	0.49	2134.78	563.91	252.42	2629.87	976.43	596.48
0.58	0.66	2119.16	566.14	250.33	2604.64	974.60	594.10
0.50	0.63	2121.80	560.88	249.06	2616.69	969.57	592.16
0.53	0.34	2115.52	585.74	260.70	2608.39	996.45	603.13
(SD/Mean)% >		0.47	1.57	1.70	0.48	0.95	0.68

Table 3. Translation invariants computed from the gray-level image “Letter A” with 10% noise.

Centroid		Geometric Moments			Schlick's Approximation		
\hat{X}	\hat{Y}	μ_{20}	μ_{13}	μ_{42}	$\tilde{\mu}_{20}$	$\tilde{\mu}_{13}$	$\tilde{\mu}_{42}$
0.52	0.52	2873.77	865.95	417.83	3453.60	1332.77	844.84
0.53	0.56	2889.17	876.26	414.42	3465.83	1339.38	844.69
0.51	0.49	2916.40	899.48	439.47	3504.43	1369.10	870.44
0.55	0.60	2879.08	906.06	419.28	3446.24	1360.25	852.65
0.50	0.59	2856.42	873.79	406.76	3444.14	1327.05	835.34
0.52	0.40	2868.74	955.06	456.17	3448.78	1411.70	881.11
(SD/Mean)% >		0.72	3.66	4.34	0.66	2.32	2.04

to compare the amount of variance between moments of different orders. The effect of Schlick's approximation on Hu's rotation invariants was studied by rotating the “Ant” image continuously from 0 to 360° in steps of 10°, and calculating the central moments using (5) and (14). The plots of rotation invariants $\mu_{20} + \mu_{02}$ and $\tilde{\mu}_{20} + \tilde{\mu}_{02}$ with respect to the angle of rotation are given in Figs. 7 and 8, respectively. The percentage variation of standard deviation over mean was found to be 0.2% for $\mu_{20} + \mu_{02}$ (Fig. 7), but this value increased to 1.29% when Schlick's approximation was used (Fig. 8). It may be noted here that $\tilde{\mu}_{20} + \tilde{\mu}_{02}$ is not a true rotation invariant, but only a modified version of Hu's invariant.

Table 4 shows the percentage of variation of Hu's invariants for a complete rotation of the “Tool” image.

Table 5 shows the values of scale invariants given by Eqs. (6) and (16), computed using the “Aircraft” image. The image is scaled uniformly by a factor α in both x - and y -directions, and a 2% salt-and-pepper-noise added. The results of a similar analysis of scale invariance of moments using the “Bird” image are given in Table 6.

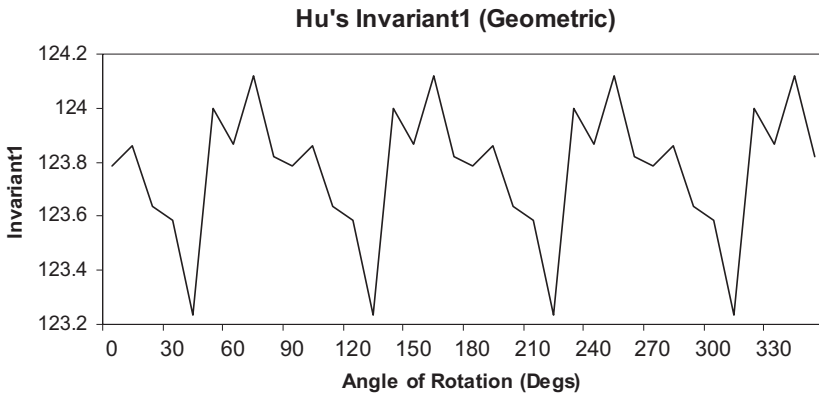


Fig. 7. Variation of first Hu's invariant with respect to angle of rotation.

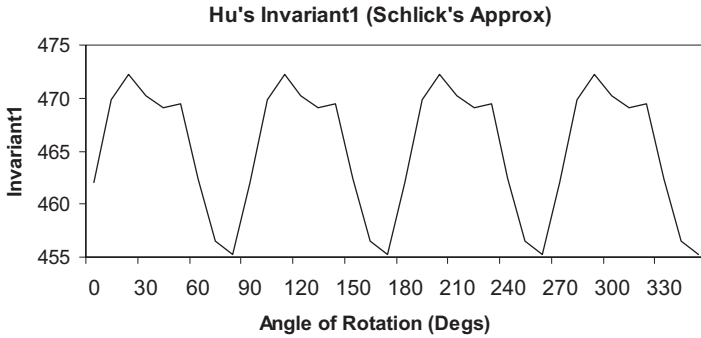


Fig. 8. Variation of first Hu's invariant computed using Schlick's approximation.

Table 4. Percentage variation of Hu's invariants computed from the "Tool" image.

Rotation Invariant	Geometric Moments (SD/Mean)%	Schlick's Approximation (SD/Mean)%
Hu's Invariant 1	2.62	4.01
Hu's Invariant 2	6.98	11.21
Hu's Invariant 3	5.17	8.84
Hu's Invariant 4	7.83	12.18
Hu's Invariant 5	9.12	12.66

Table 5. Values of scale invariant moment functions for different image scale factors, computed using the binary image "Aircraft".

Scale Factor	Geometric Moments			Schlick's Approximation			
	α	η_{30}	η_{22}	η_{14}	$\tilde{\eta}_{30}$	$\tilde{\eta}_{22}$	$\tilde{\eta}_{14}$
1		0.1836	0.0864	0.1236	0.2869	0.1321	0.2393
0.8		0.1949	0.0901	0.1360	0.2950	0.1343	0.2479
0.5		0.2089	0.0959	0.1535	0.2994	0.1384	0.2546
1.2		0.1816	0.0857	0.1195	0.2866	0.1316	0.2378
1.8		0.1931	0.0882	0.1289	0.2943	0.1347	0.2444
2		0.2006	0.0895	0.1368	0.2989	0.1354	0.2492
(SD/Mean)% >		5.3141	4.1050	9.0796	1.9132	1.8351	2.5916

The corresponding results for the gray-level image "Bird" are given in Table 6. As in the case of translation invariants, scale invariants computed using Schlick's approximation showed less variation with changes in scale factor.

We conclude the experimental analysis section with the results of a character recognition task where a feature vector comprising of the first four Hu's invariants was used to identify translated, scaled and rotated images of the letter "A". The database contained the feature vectors computed for normalized images of all 26 upper-case letters of the alphabet. The matching of feature vector was done using a simple Euclidean distance as the similarity measure. The following table gives

Table 6. Values of scale invariant moment functions for different image scale factors, computed using the gray-level image “Bird”.

Scale Factor	Geometric Moments			Schlick’s Approximation		
α	η_{30}	η_{22}	η_{40}	$\tilde{\eta}_{30}$	$\tilde{\eta}_{22}$	$\tilde{\eta}_{40}$
1	0.2526	0.1113	0.2031	0.3248	0.1489	0.2839
0.8	0.2045	0.0906	0.1477	0.2926	0.1322	0.2464
0.5	0.1558	0.0726	0.0945	0.2653	0.1186	0.2162
1.2	0.2544	0.1118	0.2051	0.3259	0.1493	0.2852
1.8	0.2602	0.1119	0.2117	0.3297	0.1492	0.2896
2	0.2622	0.1113	0.2139	0.3312	0.1487	0.2913
(SD/Mean)% >	18.5209	16.2440	26.9434	8.6137	9.1608	11.4215

Table 7. A comparison of the percentage of correctly recognized test images under varying transformation parameters and input noise.

Input Noise (%)	Geometric Moment Invariants	Moment Invariants with Schlick’s Approximation
0	93	91
2	94	89
5	88	81
10	78	74

the number of times the test image was correctly recognized for 100 test cases with different combinations of transformations (chosen randomly) and levels of input noise.

7. Conclusions

This paper has presented a modified version of geometric moments, replacing the monomial in normalized coordinates with Schlick’s approximation for each exponential term. The paper has also presented both translation and scale invariants of the modified moments and analyzed their performance with parametric variations and input noise. Schlick’s approximation is useful in significantly reducing the computational time required for evaluating the moment kernel. Coordinate normalization provides better numerical stability and robustness with respect to noise. The separability and continuous differentiability properties of the kernel function are not affected by this approximation, and therefore methods employing these properties for further reduction of computations can also be applied to the modified moments. The moment definition can be easily extended to three dimensions. The modified moments have a better dynamic range of values, particularly for high orders, compared to normalized geometric moments.

Experimental results have shown that translation and scale invariants constructed using Schlick’s approximating functions perform better compared to geometric moment invariants. The invariant characteristics of these modified moments

could also be theoretically verified. However, rotation invariants based on the new moments showed larger variation with respect to changes in angle of rotation. The rotation invariant properties of the algebraic invariants are not exactly preserved when the approximating functions are used in the moment kernel. Even though rotation invariant feature vectors can also be constructed by normalizing the image using first- and second-order moments, it is often desirable to have algebraic invariants such as those proposed by Hu.⁵ Further research in this area is directed towards the analysis of errors in Hu's rotation invariants introduced by Schlick's approximation, and the derivation of new invariant functions that are suitable for the modified kernel. An alternative method that could be looked at is the hybrid approach where low order moments (say, when $p < 20$) are computed based on the monomial kernel, while higher order moments are computed using Schlick's approximation functions. In this case, we can get both the computational speed of Schlick's approximations and also the accuracy of low order rotation invariants such as Hu's moments.

References

1. X. Bresson, P. Vanderghenst and J. P. Thiran, Geometric moments in scale spaces, *Proc. 16th Int. Conf. Patt. Recogn.* **2** (2002) 418–421.
2. J. Flusser and T. Suk, Pattern recognition by affine moment invariants, *Patt. Recogn.* **26** (1993) 167–174.
3. F. Ghorbel, S. Derrode, S. Dhahbi and R. Mezhoud, Reconstructing with geometric moments, *Proc. Int. Conf. Machine Intelligence: ACIDCA-ICMI'05* (2005).
4. F. Ghorbel *et al.*, Image reconstruction from a complete set of similarity invariants extracted from complex moments, *Patt. Recogn. Lett.* **27** (2006) 1361–1369.
5. M. K. Hu, Visual pattern recognition by moment invariants, *IRE Trans. Inform. Theor.* **8** (1962) 179–187.
6. A. Khotanzad and Y. H. Hong, Invariant image recognition by zernike moments, *IEEE Trans. Patt. Anal. Mach. Intell.* **12** (1990) 489–497.
7. J. G. Leu, Computing a shape's moments from its boundary, *Patt. Recogn.* **24**(10) (1991) 949–957.
8. B. Li, High-order moment computation of gray level images, *IEEE Trans. Imag. Process.* **4** (1995) 502–505.
9. J. Martinez, J. M. Porta and F. Thomas, A matrix-based approach to the image moment problem, *J. Math. Imag. Vis.* **26** (2006) 105–113.
10. J. Martinez and F. Thomas, Efficient computation of local geometric moments, *IEEE Trans. Imag. Process.* **11** (2002) 1102–1111.
11. R. Mukundan, Estimation of quaternion parameters from two-dimensional image moments, *Graph. Mod. Imag. Process.* **54** (1992) 345–350.
12. R. Mukundan, S. H. Ong and P. A. Lee, Image analysis by Tchebichef moments, *IEEE Trans. Imag. Process.* **10** (2001) 1357–1364.
13. R. Mukundan and K. R. Ramakrishnan, *Moment Functions in Image Analysis — Theory and Applications* (World Scientific, 1998).
14. G. Schaefer, S. Y. Zhu and B. Jones, Retrieving thermal medical images, *Proc. Int. Conf. Computer Vision and Graphics: ICCVG* (2004), pp. 906–911.
15. C. Schlick, A fast alternative to Phong's specular model, in *Graphics Gems IV*, ed. P. S. Heckbert (Elsevier Science, 1994), pp. 385–387.

16. P. Shirley, B. Smits, H. Hu and E. Lafortune, A practioner's assessment of light reflection models, *Proc. 5th Pacific Conf. Computer Graphics and Applications* (1997), pp. 40–49.
 17. C. H. Teh and R. T. Chin, On image analysis by the methods of moments, *IEEE Trans. Patt. Anal. Mach. Intell.* **10** (1988) 496–513.
 18. C. H. Wu, S. J. Horng and P. Z. Lee, A new computation of shape moments via quadtree decomposition, *Patt. Recogn.* **34** (2001) 1319–1330.
 19. L. R. Yang and F. Albrechtsen, Fast and exact computation of cartesian geometric moments using discrete Green's theorem, *Patt. Recogn.* **29** (1996) 1061–1073.
 20. P. T. Yap, R. Paramesran and S. H. Ong, Image analysis by Krawtchouk moments, *IEEE Trans. Imag. Process.* **12** (2003) 1357–1364.
 21. J. Zhou *et al.*, Image analysis by discrete Hahn moments, *Proc. Int. Conf. Imag. Analysis and Recognition: ICIAR* (2005), pp. 524–531.
-



R. Mukundan received his Ph.D degree from the Indian Institute of Science, Bangalore, India in 1996, for his research work on “Image based attitude and position estimation using moment functions”. He worked

as a senior scientist in the Control Systems Group at the Indian Space Research Organization (ISRO Satellite Centre, Bangalore, India) from 1982 to 1997. He was with the Faculty of Information Science and Technology at the Multimedia University (MMU) in Melaka, Malaysia from 1997 to 2002. He is currently a senior lecturer in the Department of Computer Science at the University of Canterbury in New Zealand.

His primary research interests are in the areas of pattern recognition, computer vision, image and video compression, and computer graphics. He has authored a research monograph titled *Moment Functions in Image Analysis — Theory and Applications* published by World Scientific, Singapore in 1998.